Optics Letters

Parity-time-symmetric coupled microring lasers operating around an exceptional point

H. Hodaei,[1] M. A. Miri,[1] A. U. Hassan,[1] W. E. Hayenga,[1] M. Heinrich,[1,2] D. N. Christodoulides,[1] and M. Khajavikhan[1,*]

[1]CREOL, The College of Optics and Photonics, University of Central Florida, Orlando, Florida 32816-2700, USA
[2]Institute of Applied Physics, Abbe Center of Photonics, Friedrich-Schiller-Universität Jena, Max-Wien-Platz 1, 07743 Jena, Germany
*Corresponding author: mercedeh@creol.ucf.edu

Received 24 July 2015; accepted 14 September 2015; posted 21 September 2015 (Doc. ID 246687); published 22 October 2015

The behavior of a parity-time-symmetric coupled microring system is studied when operating in the vicinity of an exceptional point. Using the abrupt phase transition around this point, stable single-mode lasing is demonstrated in spectrally multimoded microring arrangements. © 2015 Optical Society of America

OCIS codes: (140.3570) Lasers, single-mode; (140.3560) Lasers, ring; (130.2790) Guided waves.

http://dx.doi.org/10.1364/OL.40.004955

The notion of parity-time (PT) symmetry was first introduced within the context of mathematical physics [1]. It generally implies that even non-Hermitian systems can support entirely real spectra, provided their corresponding Hamiltonians commute with the PT operator. In recent years, several studies have shown that PT-symmetric structures can be readily realized in photonic arrangements by exploiting the mathematical isomorphism between the quantum-mechanical Schrödinger equation and the paraxial wave equation of optics [2–7]. In this regard, a necessary, albeit not sufficient, condition for optical PT symmetry to hold is that the refractive-index distribution involved should respect the relationship $n^*(-\boldsymbol{r}) = n(\boldsymbol{r})$. In other words, the real part of the complex refractive-index profile associated with a photonic PT-symmetric structure must be an even function of position, while its imaginary component representing gain or loss must have an odd distribution.

By virtue of their non-Hermiticity, PT-symmetric arrangements are capable of supporting exceptional points in their parameter space. Exceptional points, also known as non-Hermitian degeneracies, typically occur in nonconservative physical systems. At these points, the eigenvectors, as well as their associated eigenvalues, coalesce, resulting in an abrupt phase transition that dramatically changes the behavior of the system [8]. In optical settings, such degeneracies can arise from the interplay of gain and loss in the underlying design. A multitude of recent theoretical and experimental studies have shown different ways of how the presence of exceptional or phase-transition points can be fruitfully utilized to attain new behavior and functionality in non-Hermitian photonic systems, including those respecting PT symmetry [2–18]. Thus far, this methodology has been explored in a number of laser studies in which a lower threshold and an inverse pump dependence of the output power have been investigated [19–25]. Recently, the selective breaking of PT symmetry has also been considered for laser mode-management applications [24,25]. In particular, in [25], a PT-symmetric double-ring configuration was proposed as a promising avenue to enforce single-longitudinal-mode operation in inherently multimoded semiconductor microcavities. This type of system is comprised of two identical ring resonators, where one provides gain while its counterpart is subjected to an appropriate amount of loss.

In this work, our goal is to experimentally characterize the behavior of a PT-symmetric photonic molecule around the exceptional point. We start with developing a mathematical model for a coupled-cavity arrangement showing the emergence of an exceptional point as a result of increasing the gain–loss contrast between the two constituent resonators. We adopt active coupled microring resonators, depicted in Fig. 1, as a platform to perform the related experiments. The coupling strength between the rings is experimentally characterized by examining their emission spectra under uniform pumping. We then pump the rings differentially and monitor the evolution of their emission spectra as the system transitions through an exceptional point. Finally, we show that by properly adjusting the coupling strength as well as gain–loss contrast, an inherently multimoded microring arrangement can be forced to operate in a single longitudinal resonance. Furthermore, by

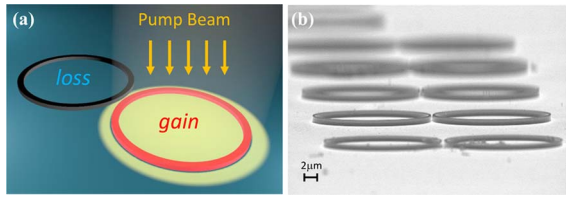

Fig. 1. (a) Schematic of a PT-symmetric microring laser. The pump beam is selectively withheld from one of the rings using a knife-edge. (b) Scanning electron-microscope image of a typical set of microring resonator pairs with different separations at an intermediate fabrication step.

simply adjusting the ambient temperature, we achieve more than 3 nm continuous wavelength tuning.

Figure 1(a) shows a coupled microring arrangement. In our current analysis, the rings' dimensions (radii, widths, and heights) are selected so as to favor the transverse electric polarization while supporting a single transverse mode in the radial direction. The coupling between the two rings is dictated by the mutual overlap of their respective modal fields throughout the interaction region and is set by their separation. The eigenfrequencies associated with the supermodes of a double-microring system as depicted in Fig. 1 can be determined through a temporal coupled-mode analysis. By considering the nth longitudinal mode in these two rings, one finds that

$$\omega_n^{(1,2)} = \omega_n + i\left(\frac{\gamma_{a_n} + \gamma_{b_n}}{2}\right) \pm \sqrt{\kappa_n^2 - \left(\frac{\gamma_{a_n} - \gamma_{b_n}}{2}\right)^2}, \quad (1)$$

where $\omega_n^{(1,2)}$ represents the eigenfrequencies of the two supermodes of this system, ω_n is the nth longitudinal resonance frequency of an isolated passive ring, γ_{a_n} and γ_{b_n} represent the net gain (positive) or loss (negative) in each ring, and κ_n stands for the coupling factor.

When both rings are subject to the same level of gain or loss ($\gamma_{a_n} = \gamma_{b_n}$), Eq. (1) reveals that the real parts of the eigenfrequencies split by $2\kappa_n$, while their imaginary components remain degenerate. As a result, a uniform pumping scheme can be used to experimentally measure the coupling strength. According to Eq. (1), an interesting situation arises when one of the rings is subject to gain while the other one is subject to the same amount of loss ($\gamma_{b_n} = -\gamma_{a_n}$). In this case, depending on the relationship between the strength of coupling ($2\kappa_n$) and the gain–loss contrast ($|\gamma_{a_n} - \gamma_{b_n}|$), the splitting either takes place in the real domain or along the imaginary axis. In particular, when the gain–loss contrast between the rings exceeds the coupling ($|\gamma_{a_n} - \gamma_{b_n}| \geq 2\kappa_n$), the real parts of the eigenfrequencies coalesce while the imaginary components lose their degeneracy. The point at which the two eigenfrequencies and their respective eigenvalues fuse ($|\gamma_{a_n} - \gamma_{b_n}| = 2\kappa_n$) is better known as an exceptional point and marks the threshold for PT-symmetry breaking [2–4].

Figure 2 illustrates the trajectories of the eigenfrequencies associated with the aforementioned coupled-microcavity system in the complex domain as they transition through an exceptional point. In this example, we start with an equally pumped coupled microring arrangement entailing two modes separated by $2\kappa_n$ along the real frequency axis. As one gradually reduces the gain in one of the resonators and replaces it with loss while the other ring is kept fixed at the initial gain level, the splitting of the resonant frequencies in the real domain monotonically decreases. At the same time, the imaginary components of the eigenfrequencies are reduced due to the lower available net gain. Nevertheless, the imaginary parts of both eigenfrequencies remain equal, indicating that the supermodes are evenly distributed between the two rings. This trend continues until the system reaches the exceptional point. At this juncture, the eigenfrequencies become fully identical in both their real and imaginary parts. Beyond this point and as the gain in the second ring is further reduced, the resonant frequency of the two modes become degenerate, while the imaginary parts bifurcate. These changes reflect the fact that in the broken-symmetry regime, one of the supermodes primarily resides in the gain region (therefore experiencing more amplification) while the other one mainly occupies the lossy ring (hence attenuates).

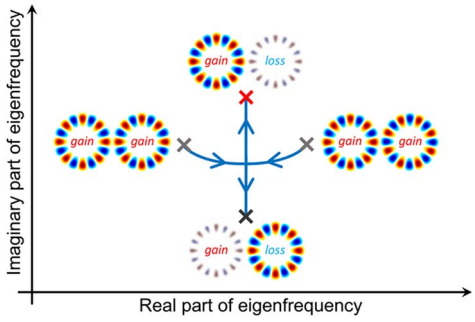

Fig. 2. Evolution of eigenfrequencies as the gain in one of the double active cavities is being gradually replaced with loss. Below the exceptional point, the eigenfrequencies split along the real axis, while keeping the same imaginary components. Above the exceptional point, the real parts of the eigenvalues merge while the imaginary parts bifurcate. At the exceptional point, the eigenfrequencies become completely identical in the complex domain.

As shown in Eq. (1), the exceptional point appears where the coupling strength between the rings becomes equal to the gain–loss contrast ($|\gamma_{a_n} - \gamma_{b_n}| = 2\kappa_n$). Consequently, an accurate measurement of the coupling factor is of fundamental importance for any subsequent investigations. To this end, we exploit the fact that the splitting $\delta\lambda$ of the resonant wavelengths in an evenly pumped pair of rings is directly related to the coupling strength through $\delta\lambda = \frac{\kappa\lambda^2}{\pi c}$ [27]. Figures 3(a)–3(d) show the lasing spectra for a system of coupled rings separated by 50, 100, 200, and 300 nm, respectively. As expected, the wavelength splitting monotonically decreases as the distance between the two rings is increased. Figure 3(e) confirms the exponential dependence of the coupling factor with respect to the spacing between the rings. For the rings separations at hand, coupling strengths on the order of $\sim 10^{12}$ per second were

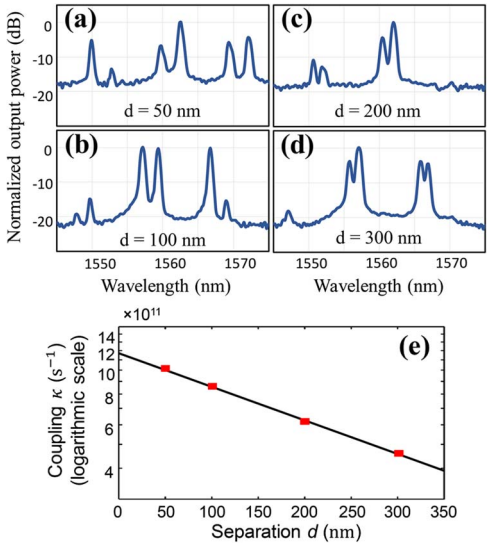

Fig. 3. (a)–(d) Lasing spectra from evenly pumped microring pairs with separations of 50, 100, 200, and 300 nm, respectively. (e) The coupling coefficient depends exponentially on the separation distance between the two rings. The resolution of the spectrometer is set at 0.4 nm.

obtained, which is in agreement with simulation results. This level of coupling requires a gain–loss contrast on the order of ~100 cm^{-1} between the rings to reach the PT-symmetry breaking point. In our arrangements, this amount of gain can be readily supplied by the InGaAsP quantum well system with pump powers in the range of a few milliwatts [28]. The variations between the magnitude of the peaks in Figs. 3(a)–3(d) can be attributed to the small detunings due to thermal and/or nonlinear mismatches between the rings [25].

Next, we study the effect of applying a nonuniform pump distribution to observe the transition of the system in the parameter space. For our subsequent experiments, we choose rings (radii: 10 μm, widths: 500 nm, heights: 210 nm) with a separation of 150 nm. Following the scheme illustrated in Fig. 2, we start with an evenly distributed pump [Fig. 4(a)] and gradually introduce loss to one of the rings by partially blocking the pump with a knife edge. Figures 4(a)–4(d) show the corresponding evolution of the output spectra. As the loss is increased, the two resonant peaks associated with the two supermodes move toward each other, while their respective intensities gradually decrease due to a reduced overall gain. A drastic change, however, happens when the system passes the exceptional point [Fig. 4(d)]. At this point, the two supermodes become spectrally degenerate and only the broken-symmetry mode with the higher Q-factor experiences sufficient amplification to lase. Video files illustrating the continuous evolution of the spectrum as well as the change in the intensity distribution are available (Visualization 1 and Visualization 2). There are two unique characteristics that distinguish this system: (i) the PT-broken mode occurs at the center of the two resonant peaks of the evenly pumped system, and (ii) the PT mode is not affected by the loss in the unpumped ring. In [25], the selective breaking of PT symmetry in double microring systems enabled by the intrinsic lineshape of the gain material has been exploited to enforce single-mode lasing in microring arrangements. Similar single-mode lasing behavior can also be observed in Fig. 4(d). As it was shown in [25], single-mode lasing can be achieved without detrimental effects on the overall lasing efficiency, since the PT-broken mode resides almost exclusively within the active ring.

Finally, we demonstrate wavelength tunability in single-mode PT lasers by utilizing the large intrinsic thermo-optical

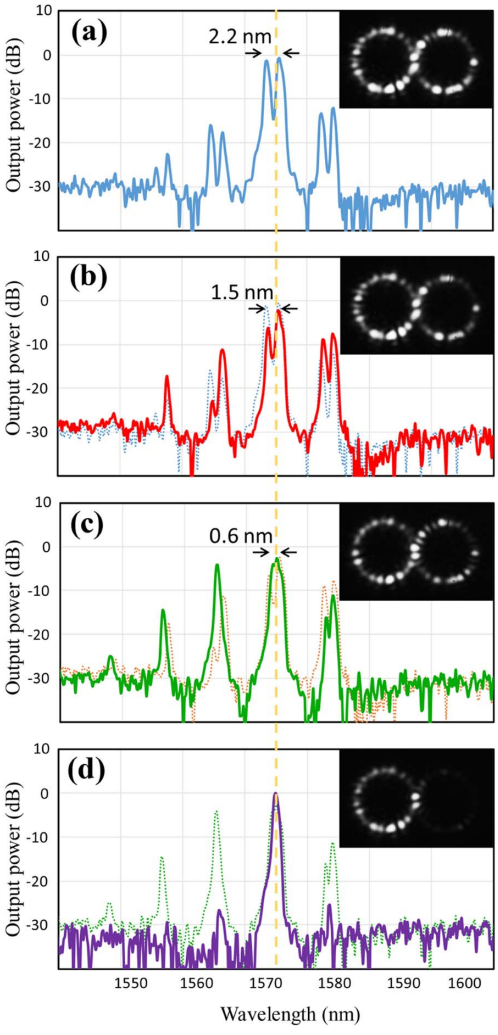

Fig. 4. Evolution of the emission spectra of a double ring structure as a knife-edge gradually covers the right ring, thus introducing loss. The insets show the intensity profile in the two rings collected from the scattered emission. The resolution of the spectrometer is set at 0.4 nm. High-resolution linewidth measurements show that the linewidth in (d) is ~10 GHz.

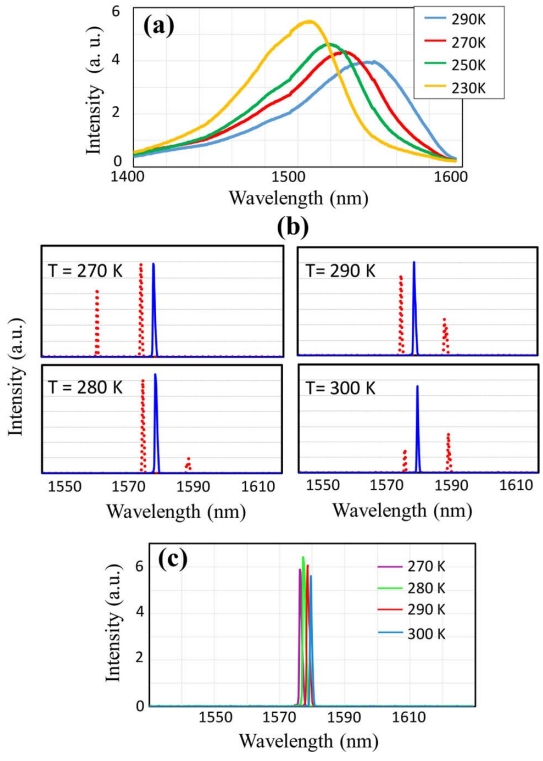

Fig. 5. Continuous wavelength tuning of a PT-symmetric single-mode microring laser. (a) Measured photoluminescence of the InGaAsP QW wafer at different temperatures. (b) Emitted spectra of the PT-symmetric laser (solid blue line) compared to single ring scenario with the same ring dimensions (dotted red line). Continuous single-mode tuning is achieved in the PT case, while the multimoded spectrum of a single ring laser undergoes severe mode hopping by changing the temperature. (c) Emitted spectrum from a PT-symmetric microring structure at temperatures of 270, 280, 290, and 300 K and pump powers of 0.8, 1, 1.4, and 1.4 mW, respectively. The observed wavelength tuning is approximately 0.1 nm K^{-1}. The rings have a radius of 6 μm and a width of 500 nm and are placed 200 nm apart from each other.

coefficient of the semiconductor gain material ($\frac{dn}{dT} \sim 10^{-4}$ K^{-1}) [29]. In a single ring configuration, the presence of multiple competing modes often leads to a discontinuous tuning because a slight shift of the amplification envelope may severely impact the ensemble of the modes involved. Figure 5(a) shows the temperature-induced shift of the photoluminescence spectrum of the quantum well active medium. Figure 5(b) compares the evolution of the emission spectra obtained from a conventional ring resonator and the PT-symmetric system as the sample temperature is externally adjusted. Interestingly, the self-adjusting properties of PT-symmetric mode stabilization seem to mitigate mode-hopping effects. Continuous spectral tuning is achieved in a PT arrangement over a range of 3.3 nm by varying the temperature between 270 and 300 K, while single-modedness is preserved with high fidelity [see Fig. 5(c)]. By further increasing the temperature, the single mode resonance jumps by a free spectral range and shifts continuously for another 3.3 nm. This is caused by the shift of the gain spectrum, as reported in Fig. 5(a), resulting in the PT-symmetry breaking to occur at a different longitudinal mode.

In conclusion, we have systematically investigated the lasing dynamics of PT-symmetric microring resonators when operating in the vicinity of an exceptional point. Our work provides insight into the role of non-Hermiticity and the characteristics of phase transitions associated with the spontaneous breaking of PT symmetry. We showed that the ring separation could be used as a design parameter in controlling the performance of a PT-symmetric microring laser. Our study provides an alternative roadmap for designing on-chip light sources, which exploit non-Hermiticity as a means to provide stability and enhanced performance in terms of single-mode operation and wavelength tunability.

Funding. National Science Foundation (NSF) (ECCS-1454531, ECCS-1128520); Army Research Office (ARO) (W911NF-14-1-0543); Air Force Office of Scientific Research (AFOSR) (FA9550-12-1-0148, FA9550-14-1-0037); German National Academy of Sciences Leopoldina (LPDR 2014-03, LPDS 2012-01).

REFERENCES

1. C. M. Bender and S. Boettcher, Phys. Rev. Lett. **80**, 5243 (1998).
2. C. M. Bender, D. C. Brody, and H. F. Jones, Phys. Rev. Lett. **89**, 270401 (2002).
3. K. G. Makris, R. El-Ganainy, D. N. Christodoulides, and Z. H. Musslimani, Phys. Rev. Lett. **100**, 103904 (2008).
4. R. El-Ganainy, K. G. Makris, D. N. Christodoulides, and Z. H. Musslimani, Opt. Lett. **32**, 2632 (2007).
5. S. Klaiman, U. Günther, and N. Moiseyev, Phys. Rev. Lett. **101**, 080402 (2008).
6. S. Longhi, Phys. Rev. Lett. **103**, 123601 (2009).
7. A. Guo, G. J. Salamo, D. Duchesne, R. Morandotti, M. Volatier-Ravat, V. Aimez, G. A. Siviloglou, and D. N. Christodoulides, Phys. Rev. Lett. **103**, 093902 (2009).
8. C. E. Rüter, K. G. Makris, R. El-Ganainy, D. N. Christodoulides, M. Segev, and D. Kip, Nat. Phys. **6**, 192 (2010).
9. A. Regensburger, C. Bersch, M. A. Miri, G. Onishchukov, D. N. Christodoulides, and U. Peschel, Nature **488**, 167 (2012).
10. S. Longhi, Phys. Rev. A **82**, 031801 (2010).
11. Y. D. Chong, L. Ge, and A. D. Stone, Phys. Rev. Lett. **106**, 093902 (2011).
12. A. Szameit, M. C. Rechtsman, O. Bahat-Treidel, and M. Segev, Phys. Rev. A **84**, 021806 (2011).
13. A. E. Miroshnichenko, B. A. Malomed, and Y. S. Kivshar, Phys. Rev. A **84**, 012123 (2011).
14. E. M. Graefe and H. F. Jones, Phys. Rev. A **84**, 013818 (2011).
15. L. Feng, Y. L. Xu, W. S. Fegadolli, M. H. Lu, J. E. Oliveira, V. R. Almeida, Y. F. Chen, and A. Scherer, Nat. Mater. **12**, 108 (2012).
16. B. Peng, Ş. K. Özdemir, F. Lei, F. Monifi, M. Gianfreda, G. L. Long, S. Fan, F. Nori, C. M. Bender, and L. Yang, Nat. Phys. **10**, 394 (2014).
17. L. Chang, X. Jiang, S. Hua, C. Yang, J. Wen, L. Jiang, G. Li, G. Wang, and M. Xiao, Nat. Photonics **8**, 524 (2014).
18. L. Feng, M. Ayache, J. Huang, Y.-L. Xu, M.-H. Lu, Y.-F. Chen, Y. Fainman, and A. Scherer, Science **333**, 729 (2011).
19. M.-A. Miri, P. LiKamWa, and D. N. Christodoulides, Opt. Lett. **37**, 764 (2012).
20. M. Liertzer, L. Ge, A. Cerjan, A. D. Stone, H. E. Türeci, and S. Rotter, Phys. Rev. Lett. **108**, 173901 (2012).
21. M. Kulishov and B. Kress, Opt. Express **21**, 22327 (2013).
22. M. Brandstetter, M. Liertzer, C. Deutsch, P. Klang, J. Schöberl, H. E. Türeci, G. Strasser, K. Unterrainer, and S. Rotter, Nat. Commun. **5**, 4034 (2014).
23. B. Peng, Ş. K. Özdemir, S. Rotter, H. Yilmaz, M. Liertzer, F. Monifi, C. M. Bender, F. Nori, and L. Yang, Science **346**, 328 (2014).
24. L. Feng, Z. J. Wong, R. M. Ma, Y. Wang, and X. Zhang, Science **346**, 972 (2014).
25. H. Hodaei, M.-A. Miri, M. Heinrich, D. N. Christodoulides, and M. Khajavikhan, Science **346**, 975 (2014).
26. M. Khajavikhan, A. Simic, M. Katz, J. H. Lee, B. Slutsky, A. Mizrahi, V. Lomakin, and Y. Fainman, Nature **482**, 204 (2012).
27. B. E. Little, S. T. Chu, H. A. Haus, J. Foresi, and J. P. Laine, J. Lightwave Technol. **15**, 998 (1997).
28. M. Rosenzweig, M. Mohrle, H. Duser, and H. Venghaus, IEEE J. Sel. Top. Quantum Electron. **27**, 1804 (1991).
29. J. Cui, Q. Miao, P. He, B. Wang, and W. Yu, "Temperature dependence of refractive index change for InGaAs/InGaAsP quantum wells," in *Conference of Information Optoelectronics, Nanofabrication and Testing* (2012).